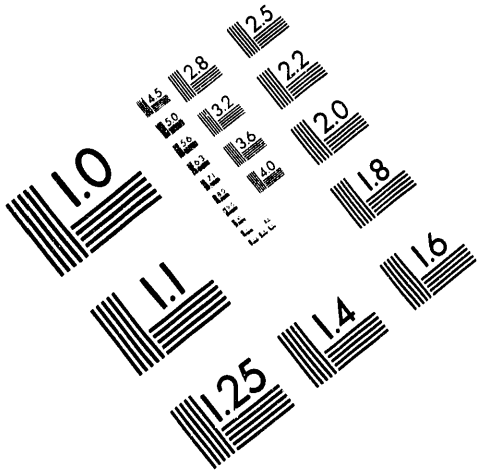

AIIM

Association for Information and Image Management

1100 Wayne Avenue, Suite 1100
Silver Spring, Maryland 20910

301/587-8202

Centimeter

Inches

MANUFACTURED TO AIIM STANDARDS
BY APPLIED IMAGE, INC.

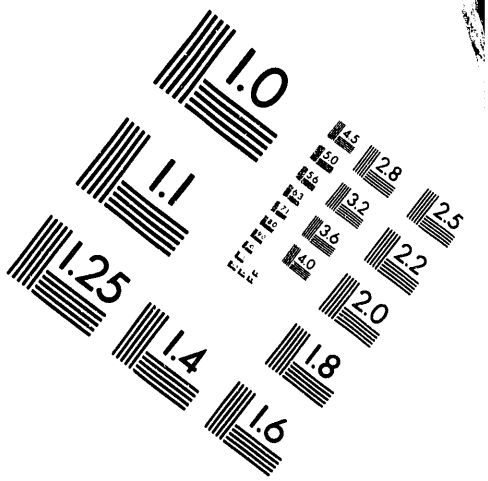

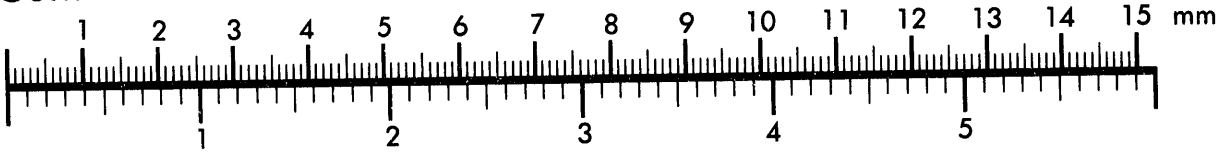

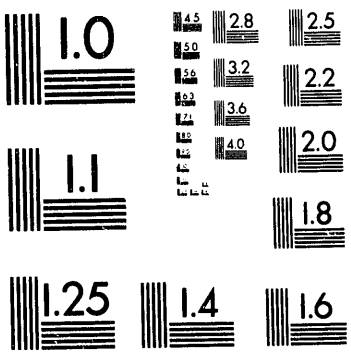

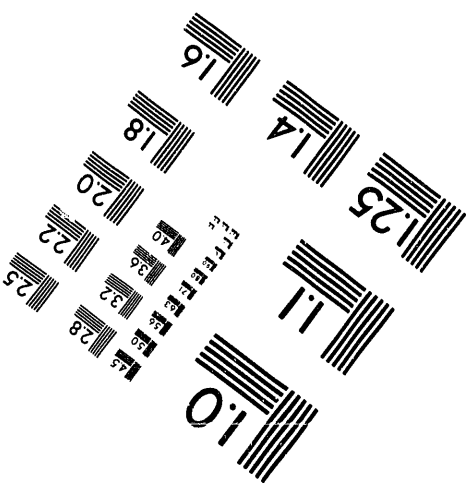

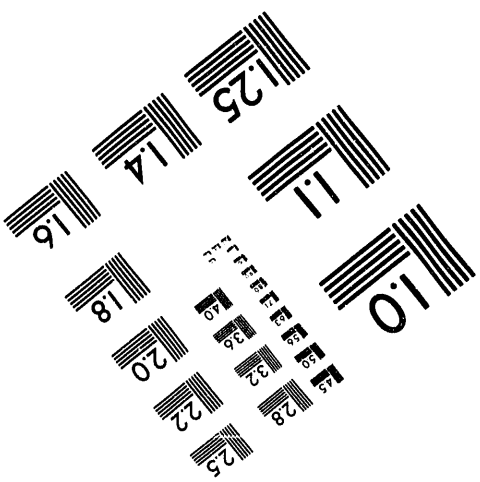

1 of 1

GA–A21312

SIMULATION OF ENHANCED TOKAMAK PERFORMANCE ON DIII–D USING FAST WAVE CURRENT DRIVE

by

J.S. deGRASSIE, Y.R. LIN-LIU, C.C. PETTY, R.I. PINSKER, V.S. CHAN, R. PRATER, H. ST. JOHN, F.W. BAITY,* R.H. GOULDING,* and D.J. HOFFMAN*

This is a preprint of an paper to be presented at the Twentieth EPS Conference on Controlled Fusion and Plasma Physics, July 26–30, 1993, Lisboa, Portugal, and to be printed in the *Proceedings.*

Work supported by
U.S. Department of Energy Contracts
DE–AC03–89ER51114 and DE-AC05–84OR21400

*Oak Ridge National Laboratory

GENERAL ATOMICS PROJECT 3466
MAY 1993

GENERAL ATOMICS

MASTER

DISTRIBUTION OF THIS DOCUMENT IS UNLIMITED

SIMULATION OF ENHANCED TOKAMAK PERFORMANCE ON DIII–D USING FAST WAVE CURRENT DRIVE*

J.S. deGrassie, Y.R. Lin-Liu, C.C. Petty, R.I. Pinsker, V.S. Chan, R. Prater, H. St.John, F.W. Baity,† R.H. Goulding,† and D.H. Hoffman†

General Atomics, San Diego, California, U.S.A.

INTRODUCTION

The fast magnetosonic wave is now recognized to be a leading candidate for noninductive current drive for the tokamak reactor due to the ability of the wave to penetrate to the hot dense core region. Fast wave current drive (FWCD) experiments on DIII–D have realized up to 120 kA of rf current drive, with up to 40% of the plasma current driven noninductively [1]. The success of these experiments at 60 MHz with a 2 MW transmitter source capability has led to a major upgrade of the FWCD system. Two additional transmitters, 30 to 120 MHz, with a 2 MW source capability each, will be added together with two new four-strap antennas in early 1994.

Another major thrust of the DIII–D program is to develop advanced tokamak modes of operation, simultaneously demonstrating improvements in confinement and stability in quasi-steady-state operation. In some of the initial advanced tokamak experiments on DIII–D with neutral beam heated (NBI) discharges it has been demonstrated that energy confinement time can be improved by rapidly elongating the plasma to force the current density profile to be more centrally peaked [2]. However, this high-ℓ_i phase of the discharge with the commensurate improvement in confinement is transient as the current density profile relaxes. By applying FWCD to the core of such a κ-ramped discharge it may be possible to sustain the high internal inductance and elevated confinement.

Using computational tools validated on the initial DIII–D FWCD experiments we find that such a high-ℓ_i advanced tokamak discharge should be capable of sustainment at the 1 MA level with the upgraded capability of the FWCD system.

DIII–D FWCD UPGRADE TO 6 MW

Figure 1 shows a schematic diagram of the FWCD system as it will be following the upgrade to a 6 MW generator source capability. That portion indicated as existing now has been described extensively [3–5]. This existing system consists of one transmitter, 2 MW, 30 to 60 MHz, driving a four-strap antenna with peak $k_{\parallel} \simeq 8.9$ m^{-1} at the antenna in current drive operation where a $\pi/2$ phase shift is set between adjacent straps.

For the upgrade portion, two new modular four-strap antennas [6,7] will be installed in DIII–D. These antennas will have partial water cooling with a power handling capability of 4 MW (each) for a 10 sec pulse. In current drive phasing the peak spectral component at the antenna is $k_{\parallel} \simeq 10$ m^{-1}. Two new transmitters will drive the two new antennas, one on each antenna initially. These transmitters are similar to those used on ASDEX–U [8], operating over 30 to 120 MHz, with a perfectly matched output power capability of 2.5 MW at the low frequency end, and 1.5 MW at the high frequency end. The power from one transmitter must be divided equally among the four straps with proper phasing between the straps. Part of the solution on DIII–D is to couple pairs of straps on an antenna into resonant loops which force these coupled straps to either be in or out of phase, depending on the length of the loops.

The transmission system will utilize the same successful techniques developed on DIII–D [3,4] for tuning and matching under current drive phasing, but with some significant improvements. An antenna decoupler [9] will be incorporated to recirculate the power coupled from one set of straps to another during operatkon with current drive phasing. This is necessary because

*This is a report of work sponsored by the U.S. Department of Energy under Contract Nos. DE-AC03-89ER51114 and DE-AC05-84OR215400.

†Oak Ridge National Laboratory, Oak Ridge, Tennessee, U.S.A.

of the mutual inductances between the straps, which otherwise results in a power imbalance in the main lines feeding the resonant loops. Another improvement will be to use phase shifters within the resonant loops, allowing the resonance frequency, and thus the operating frequency, to be changed on a shot to shot basis.

ADVANCED TOKAMAK SIMULATION

The computational tools used in this simulation are the transport code ONETWO[10] and the rf package FASTWAVE [11]. Recently ONETWO has been upgraded [12] to allow 1-1/2D transport and magnetohydrodynamic (MHD) coupled simulation calculations in which the kinetic and current profiles are evolved according to the choice of transport model; as the pressure profile evolves, the two dimensional MHD equilibrium is self-consistently calculated. In FASTWAVE the antenna spectrum is modeled by up to 20 discrete rays, with ray propagation assumed to be a straight line with a toroidal upshift. The power deposition and current drive profiles are calculated using a slab model [12], and these profiles are spread in the vertical direction by a width chosen to simulate the full-wave calculations.

The code results have been benchmarked against the experimental data on DIII–D. Figure 2 shows data from fast wave current drive experiments [1] along with the results of a code computation. The code simulations also agree with the basic scalings seen experimentally; current drive efficiency increases with electron temperature and the driven current increases with the deposited power per plasma particle, P/n.

DIII–D κ-ramp experiments have resulted in an improvement in energy confinement of 1.5 to 1.8 relative to the JET/DIII–D H–mode thermal confinement scaling [2]. In these NBI heated experiments the elongation κ is rapidly increased (200 msec) from 1.3 to 2.2 while the input power (7.5 MW) and plasma current (1 MA) are held constant. Internal inductance values of 1.8 have been obtained transiently in this manner. It is of interest to maintain this centrally peaked current profile using FWCD and test whether the enhanced confinement can be maintained noninductively.

For this FWCD-maintained high ℓ_i study we take the target plasma from the actual experimental parameters of a DIII–D κ-ramped discharge. The discharge is in the H–mode, with $n_e(0) = 5.3 \times 10^{19}$ m^{-3}, $T_e(0) = 3.9$ keV, $T_i(0) = 3.8$ keV, $Z_{eff} = 1.3$, $\kappa = 2.2$, and $\ell_i = 1.8$. The applied fast wave power is taken from the parameters of the 6 MW upgraded capability: 1.6 MW at 60 MHz on the original antenna ($n_{\parallel}$ peak $\simeq 7$) and 1.5 MW at 120 MHz on each of the two new antennas ($n_{\parallel}$ peak $\simeq 4$). Moderate NBI at 2.5 MW is also applied to provide ion heating and some additional noninductive current drive. The profiles of Z_{eff}, n_e, and χ_i are taken as those of the target plasma and held constant throughout the simulation. The electron thermal conductivity $n\chi_e$ is selected to give τ_E consistent with the enhanced confinement observed in the experiment; $n\chi_e = 5 \times 10^{19}$/m-sec. The Hirshman-Sigmar neoclassical formulation [14] is used along with a sawtooth mixing model [15]. The transport code evolves the T_e, T_i, and J profiles consistent with the calculated FW and NBI deposition profiles. As the pressure profile evolves, the 2D free boundary MHD equilibrium is self-consistently calculated.

At the end of a 2 sec FW and NBI pulse, $T_e(0) = 7.5$ keV, $T_i(0) = 4.0$ keV, and the loop voltage is nearly zero, less than 10 mV. Figure 3 shows the current profile at this time, together with the various elements making up the noninductive current drive. Table I gives a summary of the results of this simulation; FWCD is 0.37 MA ($\gamma_{FWCD} = 0.063$), NBCD is 0.09 MA, and the bootstrap current is 0.5 MA, with the remaining 0.08 MA driven Ohmically. The internal inductance has dropped to 1.4 due to current profile broadening arising from the bootstrap current at the edge.

This simulation is not an optimization of what might be obtained with the new FWCD capability. We have found similar levels of current drive for other FWCD operating scenarios, for example, for lower frequency on the new antennas. Systematic simulation parametric studies will be performed. The important result is that noninductive current drive approaching the 1 MA level, including bootstrap current, could be within reach on DIII–D next year, when the upgraded operating mode is combined with enhanced confinement resulting from an elongation ramp. The kink stability analysis for the final equilibrium is yet to be done, but from past

experience it should be stable to the $n = 1$ external kink with the DIII–D wall geometry, and unstable to a benign internal kink [16].

REFERENCES.

[1] R.I. Pinsker *et al.*, *Direct Electron Heating and Current Drive With Fast Waves in DIII–D*, in *Plasma Physics and Controlled Nuclear Fusion Research*, Proc. 14th Int. Conf. Würsburg, 1992 (International Atomic Energy Agency, Vienna, to be published).

[2] L.L. Lao *et al.*, *High Internal Inductance Improved Confinement H–Mode Discharges Obtained with an Elongation Ramp Technique in the DIII–D Tokamak*, submitted to Phys. Rev. Lett.

[3] R.I. Pinsker *et al.*, *30–60 MHz FWCD System on DIII–D: Power Division, Phase Control and Tuning for a Four-Element Antenna Array*, in Proc. 14th IEEE/NPSS Symp on Fusion Engineering, San Diego (1991), Vol. 1, p. 115.

[4] M.J. Mayberry *et al.*, *Fast Wave Current Drive Antenna Performance on DIII–D*, in Proc. 9th Top. Conf. on RF Power in Plasmas, Charleston (1991), p. 276.

[5] R.H. Goulding *et al.*, *Design and Performance of Fast Wave Current Drive Systems in the ICRF*, *ibid.*, p. 285.

[6] F.W. Baity *et al.*, *The Technology of Fast Wave Current Drive Antennas*, to be published in J. Fusion Eng. (1993).

[7] J.S. deGrassie *et al.*, *Fast Wave Current Drive System Design for DIII–D*, in Proc. 17th Symp. on Fusion Technology, Rome (1992), to be published.

[8] F. Hofmeister, *Acquisition of Technical Data and Matching Procedures for the ICRH System on ASDEX Upgrade*, *ibid.*, to be published.

[9] R.H. Goulding *et al.*, *Power Compensators for Phased Operation of Antenna Arrays on JET and DIII–D*, in Proc. 10th Top. Conf. on RF Power in Plasmas, Boston (1993), to be published.

[10] W.W. Pfeiffer *et al.*, *ONETWO: A Computer Code for Modeling Plasma Transport in Tokamaks*, General Atomics Report GA-A16178 (1980).

[11] Y.R. Lin-Liu, *Control of Current Density Profile by RF Current Drive in DIII–D*, presented at 10th Top. Conf. on RF Power in Plasmas, Boston (1993).

[12] H. St.John *et al.*, *Coupled MHD and Transport Analysis of Improved Confinement DIII–D Discharges*, this conference.

[13] S.C. Chiu *et al.*, Nucl. Fusion **29** (1989) 2175.1

[14] S.P. Hirshman and D.J. Sigmar, Nucl. Fusion **21** (1981) 1079.

[15] W.W. Pfeiffer *et al.*, *Giant Sawtooth Oscillations in the Doublet III Tokamak*, Nucl. Fusion **25** (1985) 655.

[16] A.D. Turnbull, General Atomics, private communication.

TABLE I
SIMULATION OF FWCD SUSTAINED HIGH-ℓ_i H–MODE IN DIII–D

Power		Current	
FW	4.6 MW	FWCD	0.37 MA
NB	2.5 MW	NBCD	0.09 MA
		BS	0.50 MA
		Ohmic	0.08 MA
			1.04 MA

Parameters					
a	= 0.60 m	B_T	= 2.1 T	$\beta(0)$	= 6.7%
R	= 1.70 m	n_e	= 4.6×10^{19} m^{-3}	$\langle\beta\rangle$	= 2.0%
κ	= 2.2	$\langle Z_{eff}\rangle$	= 1.8	β_N	= 2.3
ℓ_i	= 1.4	$q(0)$	= 1.0	β_p	= 2.1
I_p	= 1.0 MA	q_{95}	= 9.1	H	= 2.5

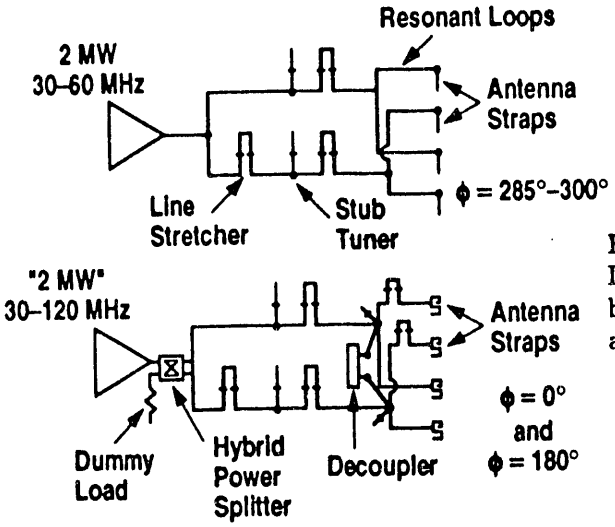

FIG. 1. (a) existing FWCD system on DIII–D; (b) two new systems like this to be added in 1994. Toroidal locations (ϕ) of antennas are given.

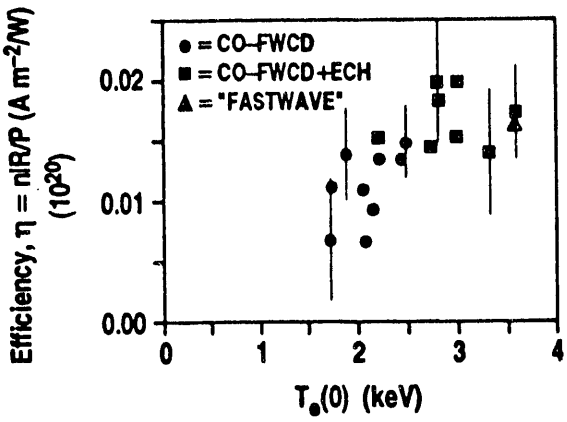

FIG. 2. Fast wave current drive efficiency versus central electron temperature. $I_p = 0.4$ MA, $B_T = 1.1$ T, $\bar{n}_e = 1 \times 10^{19}$ m^{-3}.

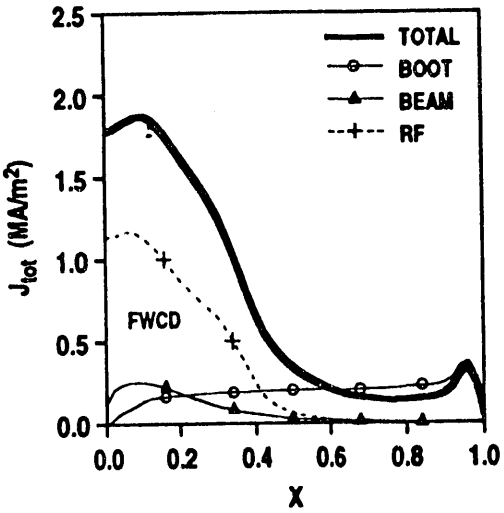

FIG. 3. Final state current density profile from simulation for FWCD applied to a κ-ramped target plasma, for coordinates of Table I.

DATE
FILMED
8/20/93

END